

## MOTIVATION

4D Magnetic Particle Imaging (MPI) reconstructions with high temporal resolution are of high relevance for diagnostic purposes.

### Dynamic concentrations

- Tracer is located in specific organs or vessels  
 ⇒ High gradients or discontinuities at organ boundaries  
 ⇒  $c(r, t)$  is discontinuous in space
- The tracer does not appear instantaneously. It accumulates, is dissipated or flows through a volume covered by one voxel  
 ⇒  $c(r, t)$  is continuously differentiable in time

### Multi-patch data

a) Multi-patch data is a concatenation of the measurements for each patch and each frame.

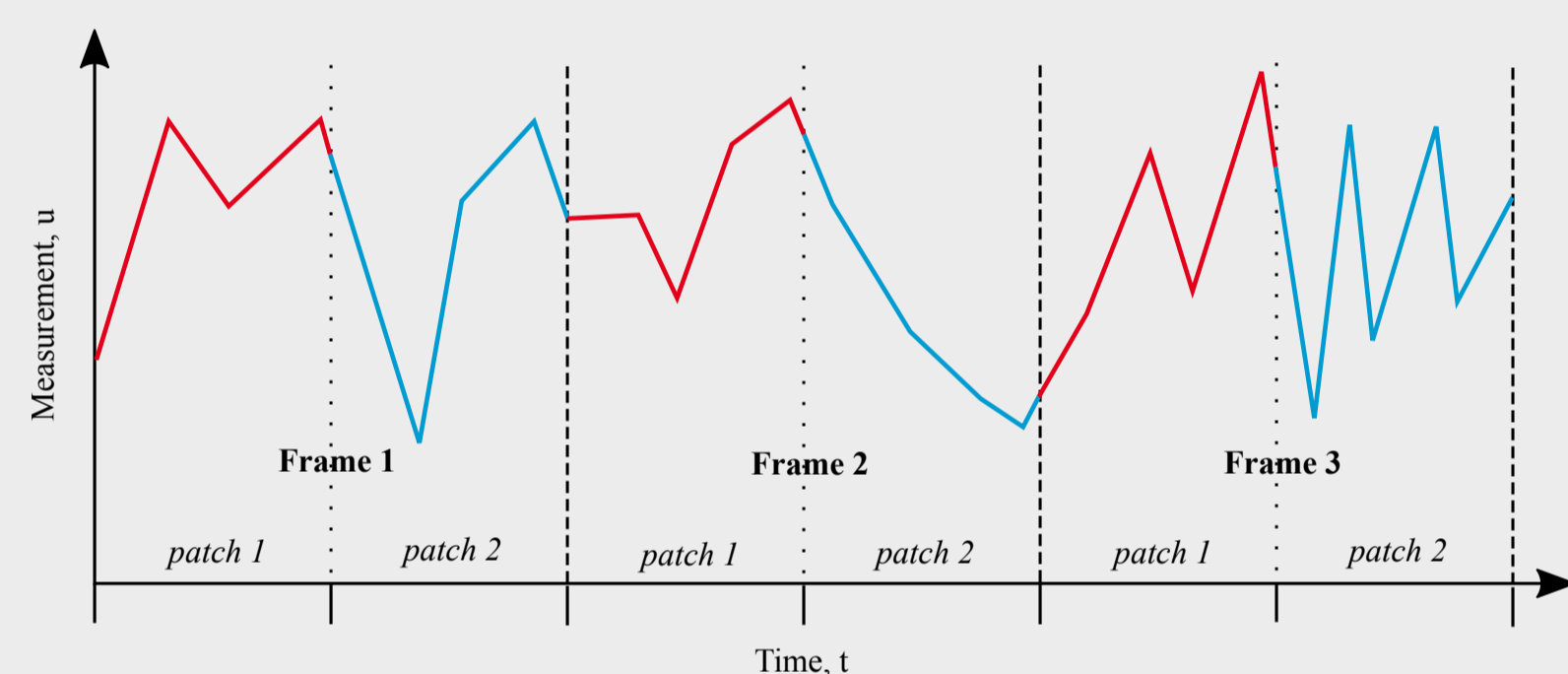


Fig. 1: The measured voltage is a concatenation of the measurements for each patch and each frame.

In between each scanning period of a patch there is at least a time span of  $T_p(P-1)$  in which the other patches are scanned ( $T_p =$  scanning time for one patch,  $P =$  number of patches).

⇒ Difficult to use similarity of subsequent frames for regularization.

b) Patches of the same frame are scanned at different time points which can cause artifacts. An extreme example is shown in the figure below.

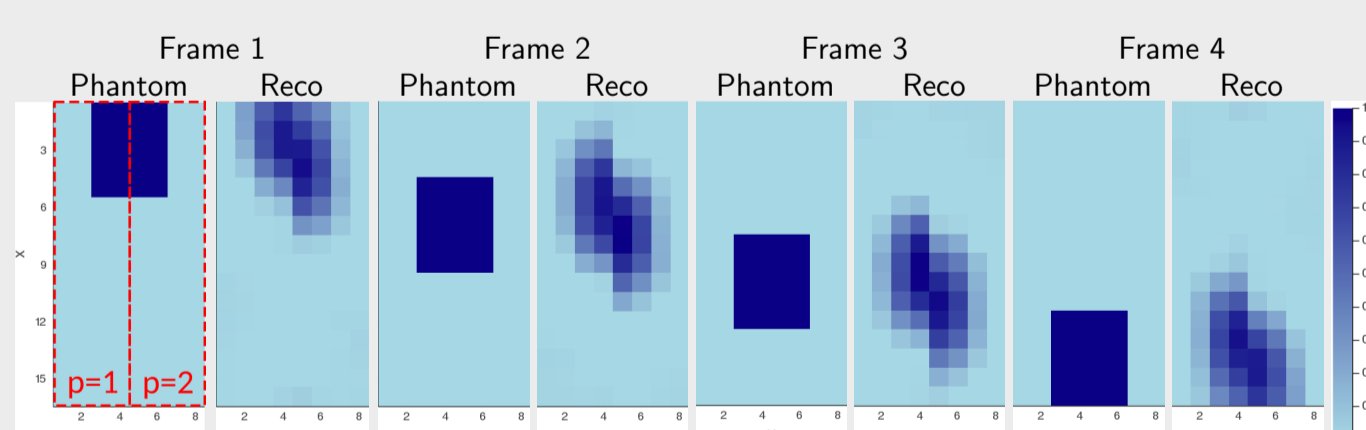


Fig. 2: Reconstruction of a 2-patch phantom with linear motion shows artefacts since the patches are scanned at different time points.

## METHODS

### Dynamic Forward Model

The MPI forward problem in time can be written as

$$u(t) = \frac{d}{dt} \int_{\Omega} c(r, t) \bar{m}(r, t) d^3r$$

which is a simplified version of the forward problem in [2] with  $c$  additionally depending on time.

Assumptions:

- Perfect filter removes signal by the excitation field
- Permeability constant can be neglected
- Coil sensitivity is constant and therefore can be neglected [2]

Dynamic tracer concentrations ⇒  $c$  is time-dependent and its time derivative is nonzero:

$$\begin{aligned}
 u(t) &= \int_{\Omega} \underbrace{\frac{d\bar{m}(r, t)}{dt}}_{S_1} c(r, t) + \bar{m}(r, t) \underbrace{\frac{dc(r, t)}{dt}}_{S_2} d^3r \\
 &= \int_{\Omega} S_1(r, t) c(r, t) + S_2(r, t) \frac{dc(r, t)}{dt} d^3r
 \end{aligned}$$

Consequences:

- New system matrix model / 2 system matrices
- Convolution in frequency domain ⇒ If possible, prefer reconstruction in time domain

### Concentration Model

Based on [1] the concentration is modeled by cubic B-splines in time for each voxel

$$c^p(r, t) = \sum_{m \in M_p} b_m(r) B_m(t), \quad \frac{dc^p}{dt}(r, t) = \sum_{m \in M_p} b_m(r) \frac{dB_m}{dt}(t).$$

$p$  is the patch index,  $b_m$  are the control points and  $B_m$  are cubic B-splines.

### Minimization Problem

Minimize

$$L(\mathbf{B}) = \sum_p \frac{1}{2} \left\| \sum_r S_1(r, t) c^p(r, t) + S_2(r, t) \frac{dc^p}{dt}(r, t) - u^p(t) \right\|_2^2$$

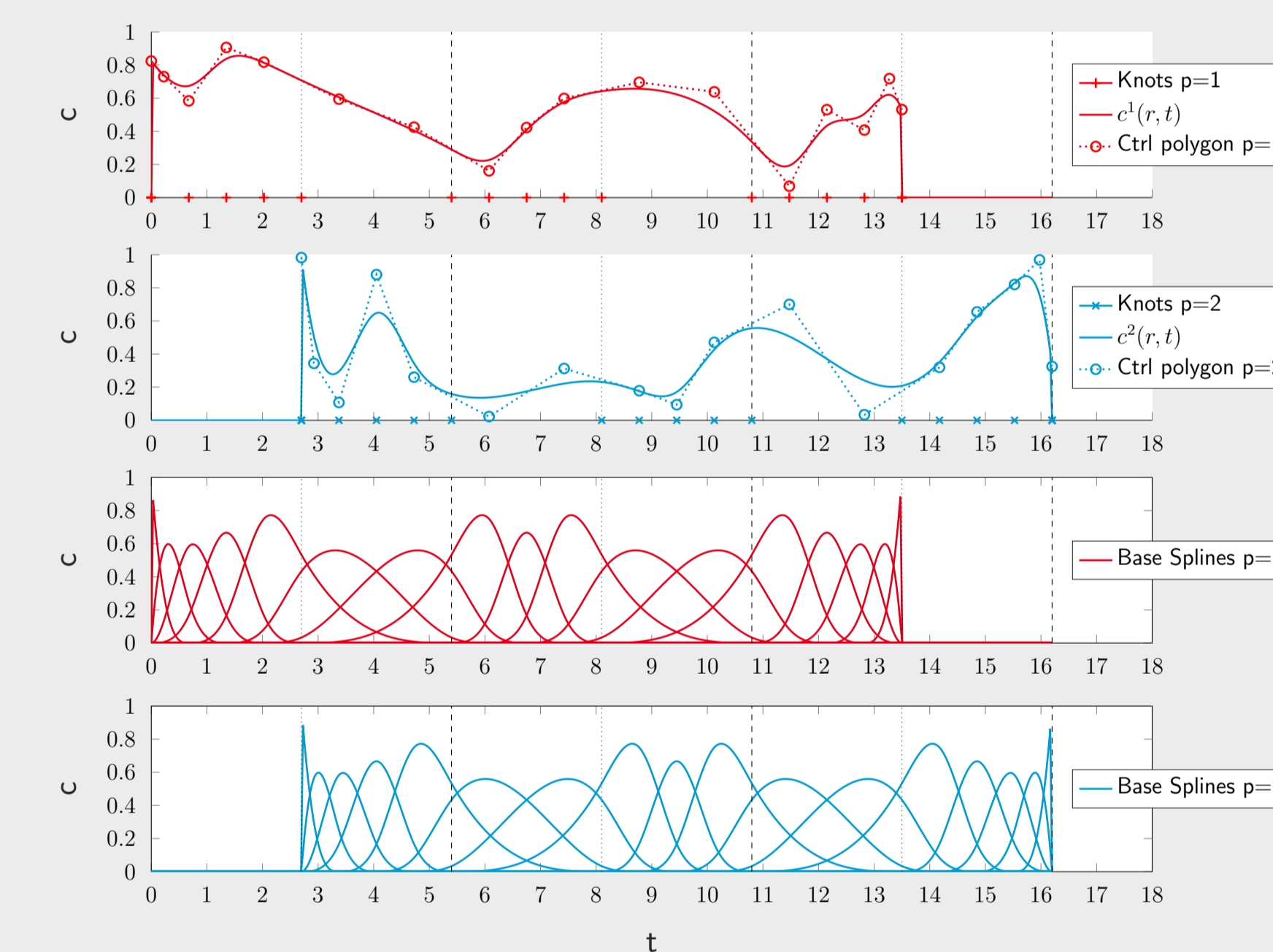
with respect to the set of all control points  $\mathbf{B} = [b_m(r)]_{m=1 \dots R, p=1 \dots P}$ .

## SPLINE SETUP

If the knots are chosen accordingly, this approach ensures differentiability in time, even for the periods without data for certain patches. Discontinuity in space is still possible as there is a specific set of control points for each voxel.

- $M_0$  uniformly distributed knots are placed in each scanning interval of the patch.
- Quadruple knots are placed at the beginning and end of the scan time for each patch to allow discontinuities at these time points.

**Example curve** for a fixed voxel  $r$ : The scan has 2 patches, 3 frames and  $M_0 = 5$ . The first and second image show the curves for the respective patches, their control polygons  $b_m(r), m \in M_p$  and the location of the knots. The third and fourth image show the respective spline basis functions  $B_m(t), m \in M_p$ .



## MINIMIZATION

As we limit the reconstructed concentrations to those representable as spline curves this provides an implicit regularization. Currently there is no other regularization applied. It can be minimized e.g. with a gradient descent. Depending on which further regularization terms are added more sophisticated algorithms might be required, e.g. a primal-dual algorithm.

## RESULTS

The algorithm was tested with simulated measurements from computational phantoms. This enables reconstructions in time domain without any filtering or post-processing steps e.g. frequency selection, spectral leakage correction. The phantom setup and behavior in time can be seen in the two figures below. There is a box within both patches. The concentration follows a spline curve such that the movement of the box is a smoothed linear motion in  $x$ -direction.

The phantom has 2 patches, with  $16 \times 4 \times 1$  voxels. The simulation measures 4 frames and 408 time points within each cycle. There is no patch overlap, no overscanning and each patch is scanned once per frame.

The minimization problem was solved with 50 gradient descent steps and  $M_0 = 5$ .  $X$ - and  $y$ -channel reconstructions were averaged to obtain the following reconstructions.

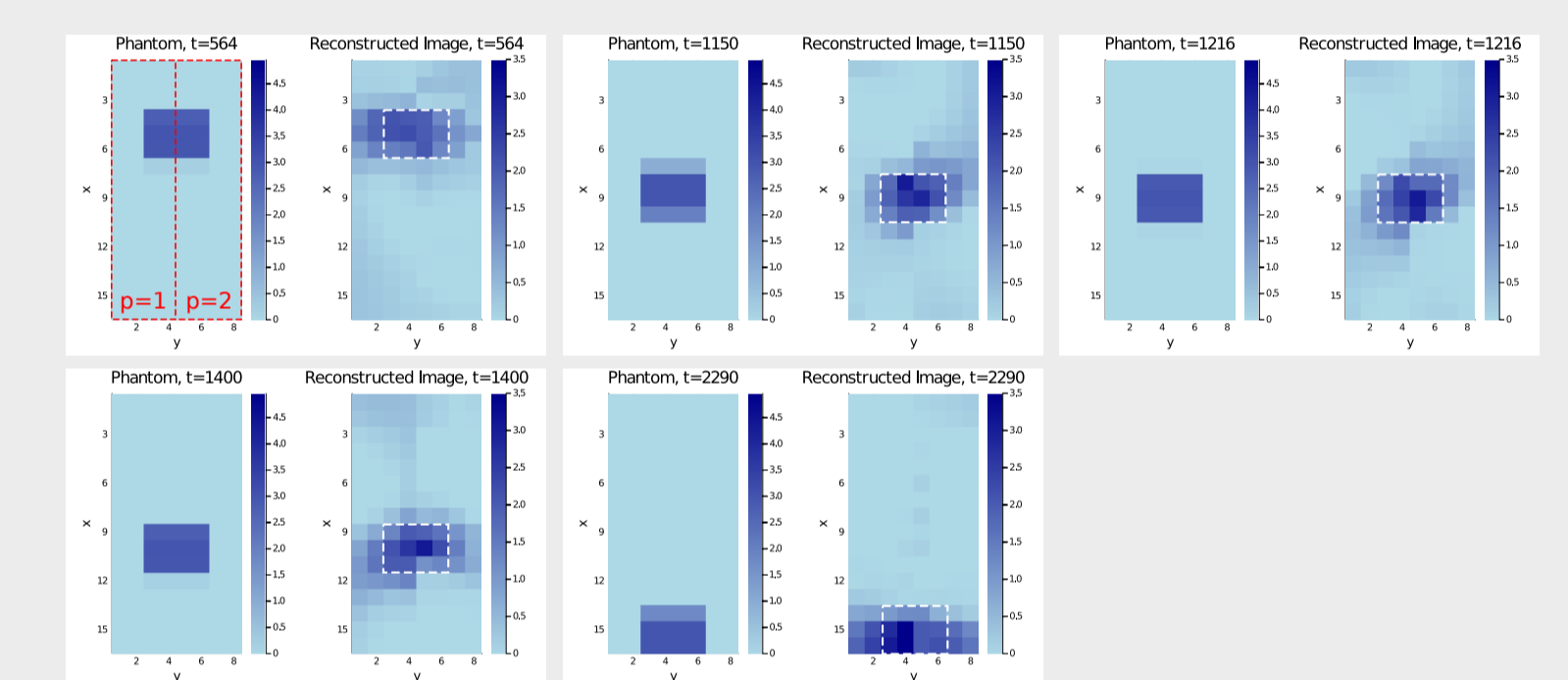


Fig. 3: Four frames of the phantom (left) and the xy-average reconstruction (right) at the same time points. The white dashed box indicates the outlines of the current position of the object in the phantom.

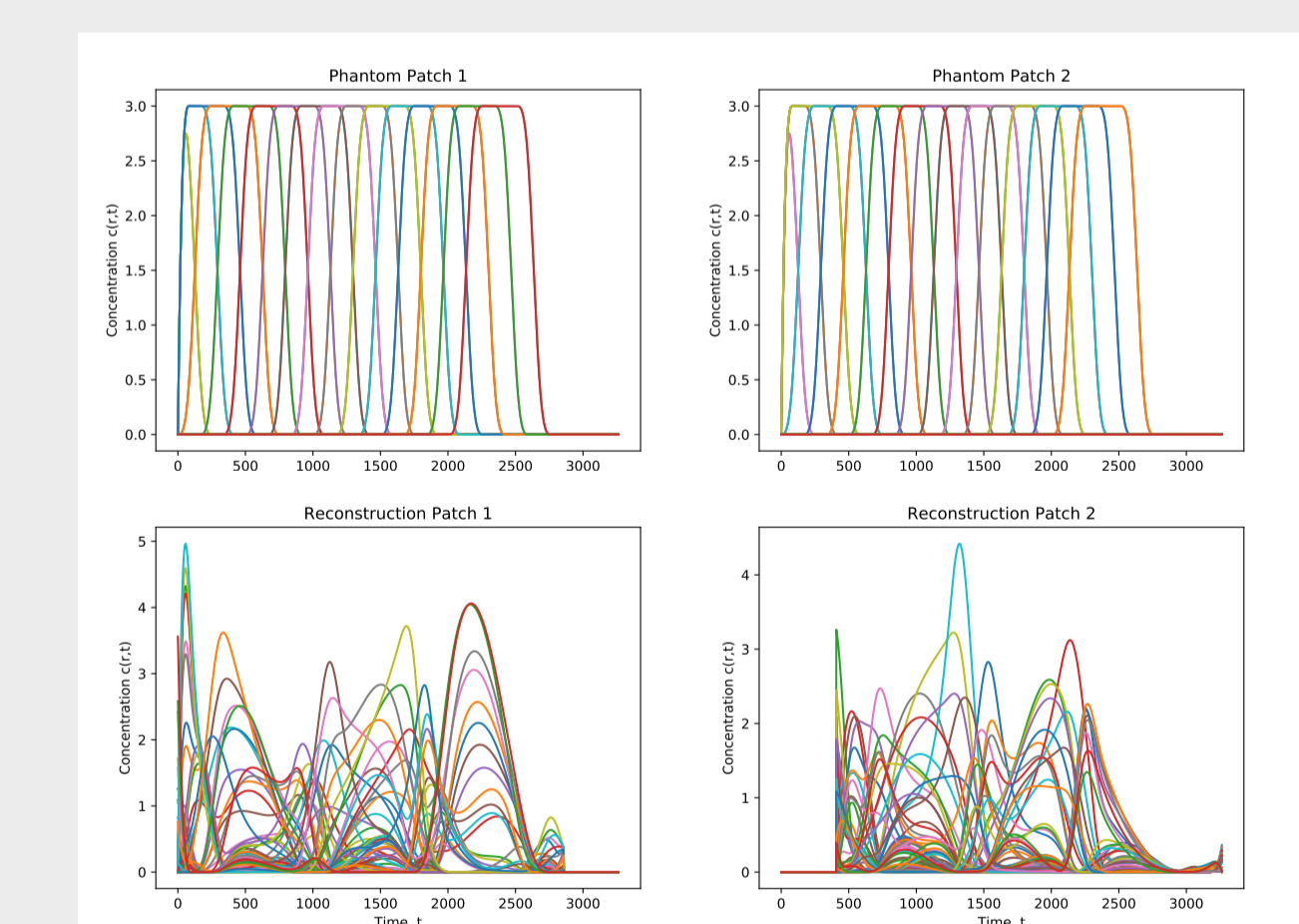


Fig. 4: Time development over the full scanning time for each voxel of each patch for the phantom (above) and the xy-average reconstruction (below). Each curve represents one voxel.

## DISCUSSION

Advantages:

- Reconstructions with infinitely high temporal resolution
- Data approximation during scanning time of other patches
- Implicit regularization
- Potential reduction of artifacts

Future work:

- Reconstruction of hybrid data: Simulate measurement with computational phantom and measured system matrix. Reconstruct with the new matrix model (and concentration model).
- Reconstruction of measured data
- Adding regularization terms e.g. sparsity in space, conservation of mass
- Using faster minimization methods

## LITERATURE

- [1] E. Gravier, Y. Yang, and M. Jin. Tomographic reconstruction of dynamic cardiac image sequences. *IEEE transactions on image processing*, 16(4):932–942, 2007.
- [2] T. Knopp and T. Buzug. *Magnetic Particle Imaging: An Introduction to Imaging Principles and Scanner Instrumentation*. Springer Berlin Heidelberg, 2012.